16th IMEKO TC10 Conference
"Testing, Diagnostics & Inspection as a comprehensive value chain for Quality & Safety
Berlin, Germany, on September 3-4, 2019

Experimental analysis of IMU under vibration

D. Capriglione[2], M. Carratu[2], M. Catelani[1], L. Ciani[1], G. Patrizi[1], R. Singuaroli[1], P. Sommella[2]

[1]Dpt. of Information Engineering, University of Florence, via di S. Marta 3, 50139, Florence (Italy)
[2]Dpt. of Industrial Engineering, University of Salerno, via di G. Paolo II 143, 84084, Fisciano (Italy)

***Abstract* – MEMS-based Inertial Measurement Units are today widely employed in many contexts. Especially in the field of self-driving vehicles and navigation they provide important information to the electronic control units for implementing positioning, localization and tracking algorithms. As a consequence, it becomes important to analyse the accuracy, reliability and time to failure of such systems when operating in conditions as more as possible similar to ones experienceable in the practice. To these aims, in this paper we investigate on IMU performance under random vibration which can be thought of as a kind of stress to which IMUs are continuously interested during their common operating. The experimental results have proved that these devices are very sensitive to the considered conditions and that suitable measurement procedures and measurement setup should be designed for the IMUs performance analysis.**

Keywords – Testing, Reliability, Accelerometer, Gyroscope, Metrological Performance, Automotive.

I. INTRODUCTION

Today, Inertial Measurement Units (IMUs) are widespread in many application contexts. Cellular phones, cars, human motion, robotics, self-driving vehicles, navigation in transportation vehicles, military and aviation represent only a part of frameworks in which these kind of devices are more and more employed [1]-[5].

Consequently, due to their wide and even increasing use in several applications, the accuracy and reliability of such systems become fundamental for assuring the expected behaviour and the correct operating of all those systems based on IMUs.

Dependently on the complexity, costs, size and weight constraints of the specific application, IMUs could integrate triaxial accelerometers (for measuring the linear acceleration), triaxial gyroscopes (for measuring the angular rate) and triaxial magnetometers (for measuring the static magnetic field) or only a subset of them.

From a practical point of view, the common solutions available today on the market, are low cost systems based on Micro Electro-Mechanical Systems (MEMS) devices [6]. Thanks to their small size, these kind of devices are easily integrated in many systems and provide measurement information for algorithms of positioning, localization and tracking to cite a few [7]-[11].

Expected performance of such systems are provided in the related datasheets by their manufacturers which, generally, consider simplified operating conditions that are not well representative of actual way of operating of such devices. Indeed, typical information that can be found in datasheets deal with selectable ranges for measuring linear acceleration, angle rate and static magnetic field, as well as the related sensitivity (to each detected quantity) and the temperature operating range. Nevertheless, the dynamic metrological performance and how the actual operating conditions can affect the metrological performance and reliability of such systems is not adequately dealt with.

Recently, some analysis have been performed to verify the influence of temperature on the performance of accelerometers and gyroscopes embedded in IMUs [12],[13] , but currently, the literature of the field seems be still lacking of performance analyses of IMUs when operating in real scenarios characterized by the presence of significant vibrations. As an example, in automotive context, in navigation and industrial environments, IMUs are continuously interested by mechanical stresses as random vibrations, so it is expected that the effects of such vibrations could generally affect both the metrological performance, the reliability and the time to failure.

Starting from these considerations, in this paper, a suitable measurement setup has been designed for analysing the effects of random vibration on commercial and very popular IMU devices. To these aims, a suitable Printed Circuit Board (PCB) has been specifically designed and realized for hosting only the device under test (DUT), the electronic circuitry and connectors needed for powering the DUT and allowing digital data exchange with the required external Micro Controller Unit (MCU). By this way, it is expected that the experimental results will depend only on DUT performance and will not be affected by any auxiliary device (MCU, data logger, user monitor and so on) adopted in the test set-up. In particular, the DUT is an IMU including one triaxial accelerometer, one triaxial gyroscope and one triaxial magnetometer.

As for the vibration test profiles, since specific standards for testing IMUs are not yet available, they have been designed and carried out by taking into account the main international standards in force applicable to MEMS devices in automotive environment.

The paper is organized as follows: section II describes the adopted DUT and the realized electronic and user interface for managing the tests, section III describes the designed test profiles, section IV shows the experimental setup, section V the achieved measurement results, and finally conclusions are reported in section VI.

II. THE DEVICE UNDER TEST

In order to test the IMU, under conditions that will be reported in section III, a suitable experimental measurement setup has been developed. It is composed by the following main parts (see Fig.1): three commercial IMU adapter boards, three satellite boards (hereinafter *Module A*, *Module B* and *Module C*, respectively) hosting the IMU adapter boards, three STM32 Nucleo-64 boards and a Raspberry PI3 equipped with an LCD. The aim of the experimental setup is to acquire data coming from three identical IMUs equally stressed by a shaker.

More in detail, the inertial platform considered is typically adopted in several applications as indoor navigation, smart user interfaces, advanced gesture recognition and automotive; it includes a 3D digital linear acceleration sensor, a 3D digital angular rate sensor, and a 3D digital magnetic sensor. About the metrological performances, the LSM9DS1 has a linear acceleration full scale of ±2g/±4g/±8/±16 g, a magnetic field full scale of ±4/±8/±12/±16 gauss and an angular rate of ±245/±500/±2000 dps. In the experimental test bed considered, the LSM9DS1 has been configured to have a scale of 16g for the accelerometer, 2000 dps for the gyroscope and 16 gauss for the magnetometer, achieving respectively a sensitivity of 0.732 mg/LSB, 0.43 mgauss/LSB, and 70 mdps/LSB. To get data from the considered adapted board, different communication protocols can be used, but in this case the SPI serial standard interface has been used.

About the satellite boards, they have been specifically designed and developed to hold the adapter boards. More in detail, the three *Modules A, B* and *C* used for the experiments have been fixed on rigid support in order to be installed at the same time on a plane for the vibrations test (see section IV). The geometry of the satellite boards has been modeled to reduce the influence of the mechanical parts to the propagation of vibrations into sensors held on them, especially to avoid the excitation of resonance frequency able to destroy or disassemble the satellite boards with the respective IMU adapter boards. Particular attention has been devoted to the orientation of the satellite boards with respect to both the LSM9DS1 inertial sensor and the fixed support in order to align the sensor axes with the shaker.

The STM32 Nucleo-64 boards [14] have been used to retrieve the data coming from the three *Modules A, B* and *C*, previously described, through a ribbon cable using an SPI communication configured to work at 10 kHz. More in detail, the STM32 Nucleo-64 board manages the configuration and communication over SPI with the inertial platform and sends the acquired data through USB to the Raspberry PI3. The firmware of the STM32 Nucleo-64 handles the data acquisition doing polling of the LSM9DS1 data-ready register. The data acquisition has been synchronized with the magnetometer ODR (Output Data Ready) since it represents the slowly peripheral among the gyroscope and accelerometer (80 Hz ODR).

The Raspberry PI3 [15] is a series of tiny single-board computers provided with all the features usually commons in a desktop computer; it has been useful in our case to acquire and store data from the inertial platform. The Raspberry PI3 is provided with a real-time operative system (Raspbian in our case) where suitable programming tools can be installed. For the aim, a Phyton console has been installed and used to contemporary store and acquire the data coming from the three Nucleo-64 boards. An SD card of 32 Gb has been used to enable the storing of a big amount of data according to the programmed test reported in section III.

A suitable LCD display with a touchscreen has been used to interact with the prototype and start the acquisition process. The data recorded during the experimentations can be extracted from the prototype thanks to variously available connections on the Raspberry PI3 as the USB port and WIFI/Ethernet port.

III. VIBRATION TEST FOR MEMS DEVICES

Both sensors and electronic devices inside automobiles and motorcycles are forced to endure extreme process and

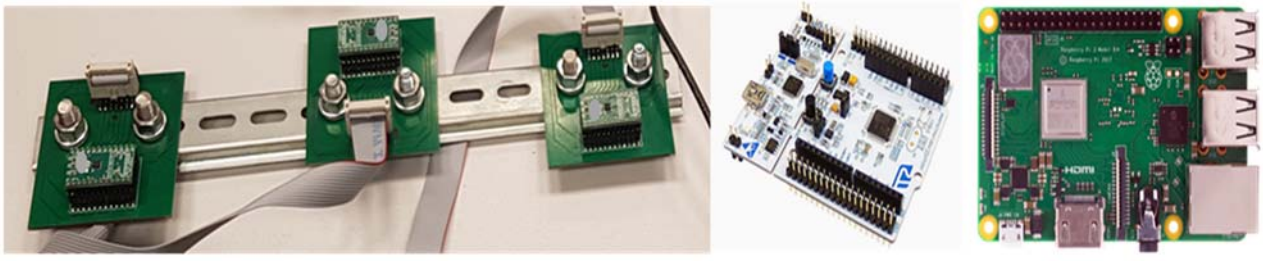

a) ***b)*** ***c)***

Figure 1. The test bed experimented, from the left to right: a) Satellite Boards (Modules A, B and C), b) Nucleo Board, c) Raspberry PI3.

environmental conditions that can generate fatigue and fracture on the devices and affect their reliability performance [16]–[18].

For this reason, the environmental characterization of the MEMS Inertial Modules based on failure analysis and experimental tests is mandatory in order to prove the device validity for automotive fields. For the failure analysis, the work focuses on the mechanical physical domain. The typical failure mechanisms of MEMS sensors are [19]-[22]:

- *Fracture* caused by overload, fatigue, shock or stress corrosion;
- *Wear* due to adhesive or abrasive contact surface, corrosion or surface fatigue;
- *Creep and plastic deformation* caused by over vibration or intrinsic stresses;
- *Stiction* due to residual stress, chemical bonding, overload or electrical static force.

A common acceleration factor that influences all the MEMS failure mechanisms is the vibration. For this reason, a random vibration test profile was specifically designed for the device under test comparing several different vibration standards and reports: IEC 60068-2-64 (2012) [23], ISO 16750-3 (2003) [24], FIAT ENS0310 (2009) [25], MIL-STD-810G (2008) [26], ETSI EN 300 019-2-5 (2002) [27] and JESD22-B103B.01 (2016) [28]. The monitoring of critical components using experimental test also allow to achieve an improvement in term of system performances, reliability and availability [29]-[30].

The random vibration test is performed to verify that the MEMS Inertial Module will function in and withstand the vibration exposures of a life cycle in automotive application. This kind of test may be used to identify accumulated stress effects and the resulting mechanical weakness and degradation in the specified performance.

Gaussian random vibration has to be applied to the component's outer surface casing or leads in a manner to simulate classical motorcycle application or expected vibration during packaged shipment. The device case shall be rigidly fastened on the vibration platform and the leads adequately secured to avoid excessive lead resonance. The components will be mounted in such a manner so that they experience the full-specified vibration level at the component [28].

Generally, the random vibration test severity is described using the acceleration spectral density (ASD), which represents "the mean-square value of that part of an acceleration signal passed by a narrow-band filter of a centre frequency, per unit bandwidth, in the limit as the bandwidth approaches zero and the averaging time approaches infinity" [23]. The random profile developed for this application is reported in Fig. 2, where both frequency and ASD are reported in logarithmic scale.

At low-frequency, the test severity is described as follow:

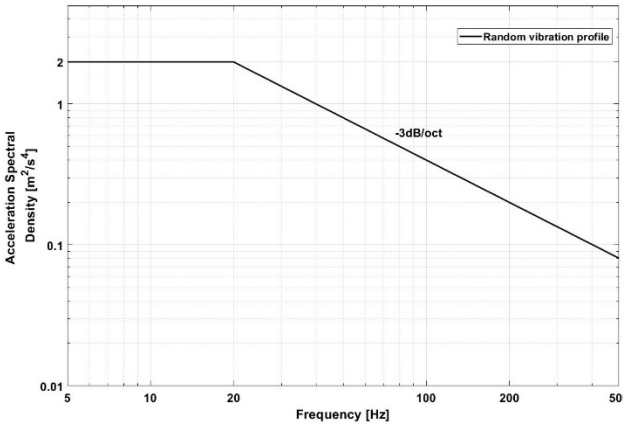

Fig.2. Random vibration profile

$$ASD = 2\frac{m^2}{s^3} = 0.02\frac{g^2}{Hz} \quad if \quad f \in [5Hz - 20Hz] \qquad (1)$$

Once overtaken the low-frequency range, the acceleration spectral density decreases as $-3dB/oct$ up to $500Hz$. The overall test level associated to the vibration profile is illustrated in Table 1. The key parameter is the Root Mean Square Acceleration G_{RMS} which represents the square root of the area under the ASD curve in the frequency domain. It is important to note that G_{RMS} contains no spectral information, therefore it cannot be used as the only constraint to define the test severity. G_{RMS} is useful in monitoring vibration tests since RMS can be monitored continuously, whereas measured spectra are available on a delayed, periodic basis.

The test will be performed for a duration of 30 minutes for each orthogonal axis, so 90 minutes in total to complete all the three axes. The ASD test level shall be applied within a tolerance $\pm 3dB$ of the nominal value at any frequency, allowing for the instrument and random error, referred to the specified ASD (see Fig. 2). The RMS acceleration levels shall not deviate more than $\pm 10\%$ of the nominal value included in Table 1. The given vibration profile was applied because it is a standard profile specifically tuned to reflect the operative condition of the device under test applied in the automotive field. Clearly, there are many other types of vibration test that could be used to characterize the performance of the IMU, like the sinusoidal profile or the step-test profile. The choice of the

Table 1. Overall measures of random vibration test level

Test Parameter	Test level
Profile Acceleration RMS	12.6197 m/s²
Profile Velocity RMS	0.0941 m/s
Profile Displacement RMS	1.8459 mm
Time for each axis	30 minutes

Table 2. Main Shaker parameters

Shaker Parameter	Max test level
Displacement Limit Peak	±25.5m
Maximum Velocity Peak	2 m/s
Maximum Acceleration Peak	2492 m/s²
Drive Frequency range	2Hz to 2000Hz

random vibration is basically due to the possibility to test the behavior of the system at different frequencies simultaneously, so other profiles are not considered in this work.

IV. EXPERIMENTAL SET-UP

The experimental tests were fulfilled at Analytical CETACE test laboratory using a Sentek M2232A shaker. The shaker main parameters are illustrated in Table 2.

Two identical *3056B2 General Purpose Accelerometer* by Dytron Instruments Inc. were used as input channel for the vibration controller. According to the manufacturer, the performances of the reference accelerometer are schematized in Table 3. The features of shaker and accelerometers allow to implement the vibration profile developed in the previous paragraph without restrictions on the severity level.

One accelerometer has to be located directly on the device under test, in such a way its output could be used as control input signal for the controller, while the other accelerometer has to be located on the shaker table. Using this configuration it is possible to control the amplitude of the vibration produced by the shaker allowing to apply the vibration profile directly on the DUT with high level of accuracy.

The fixing of the device to the shaker represents one of the most challenging steps of the vibration test, it must propagate the vibration equally to all the sections of the device under test without absorb it. Moreover, it must be safe and it must have the resonance mode out of the profile

Table 3. Accelerometer specifications

Accelerometer Parameter	Feature
Technology	Piezoelectric
Sensitivity, ±5%	100mV/g
Frequency range	1Hz to 10kHz
Electrical noise	0.0004grms
Linearity	±1% F.S.
Max vibration	±400g

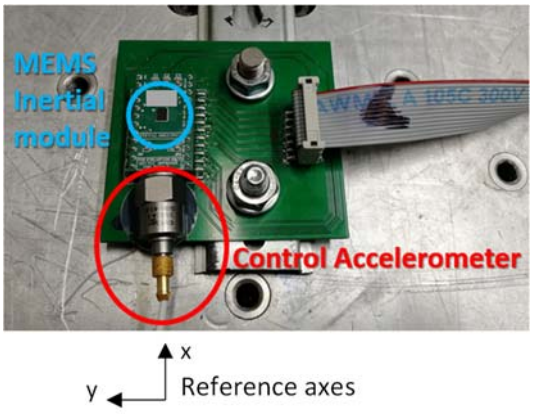

Fig.3. Experimental set-up

frequency range. Figure 3 shows the experimental set-up implemented for this test.

V. EXPERIMENTAL RESULTS

This section reports the results achieved through the experimental campaign described in the previous sections.

In particular, Figures 4 and 5 report the evolution of RMS values measured by the accelerometers and gyroscopes of *Module A* on both axes (*x* and *y*), when the shaker has actuated the vibration only along the *x*-axis (according to the reference system of Figure 3). Focusing the attention on Figures 4-5, we can identify three main zones: (i) Z_1 which corresponds to a "quite zone" in which no vibration is applied by the shaker, (ii) Z_2 which corresponds to the vibration applied according to the random profile described in section III, and (iii) Z_3 which corresponds to another "quite zone" achieved after the vibration has been stopped. As you can see, even if the vibration is actuated only on the *x*-axis, both accelerometer and gyroscope show a sensitivity also on the other axis (i.e. *y*-axis). Indeed, in Zone 2, the RMS values are significantly different from ones observed in Zone 1 and Zone 3 for both sensors axes. Similar trends have been observed for Modules *B* and *C*, here not reported for a sake of brevity.

Table 4 summarizes the achieved results for all

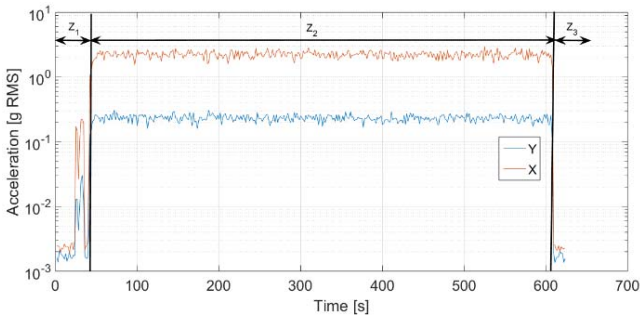

Fig.4. Module A accelerometer sensor output (the vibration is applied on the x-axis).

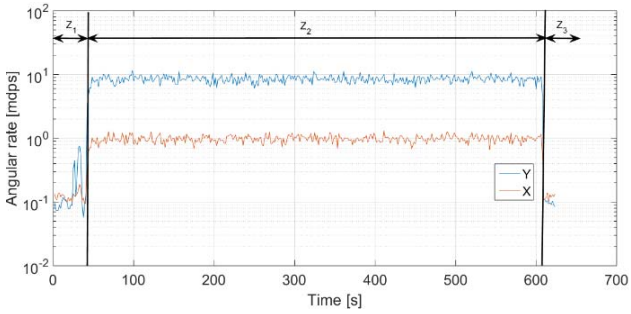

Fig.5. Module A gyroscope sensor output (the vibration is applied on the x-axis).

modules (*A*, *B* and *C*) and the two sensors axis by showing the means (μ) and standard deviations (σ) of RMS values. The following main considerations can be drawn:

- The results for Modules *B* and *C* confirm the same behaviours observed for module *A* (i.e. even if the vibration is actuated only on the *x*-axis, both Accelerometer and Gyroscope show a sensitivity also on the *y*-axis).
- As for the zones Z_1 and Z_3, whatever be either the sensor (Accelerometer or Gyroscope), the axis (*x* or *y*), and the Module (*A*, *B*, *C*) the achieved results show the experimental tests do not significantly affect the metrological performance of the considered systems. In particular, by comparing the mean RMS values (μ) observed in Z_1 and Z_3, the considered vibration tests have not lead to sensors losing calibration.
- For the zones Z_2, whatever be either the sensor (Accelerometer or Gyroscope) and the sensor axis considered (*x* or *y*), all modules show two-by-two compatible measurement results. Moreover, the RMS values measured by the sensors well-match the reference values imposed by the shaker.

VI. CONCLUSIONS

The experimental results achieved in this paper have confirmed how the vibration generally affects the operating of the considered IMUs. In particular, the application of the vibration along only one axis at a time (i.e. *x*-axis) has proved that both accelerometers and gyroscopes detect such vibration also on the unexpected axis (i.e. *y*-axis). For these reasons, measurement setup and measurement procedure for evaluating performance of such devices should take into account the need to analyse the rejection of undesired sensitivity on the not excited axis as well.

All these results also push toward the adoption of well-designed pre-processing techniques able to filter or compensate these behaviours mainly in applications where data fusions are adopted for object positioning and tracking purposes.

In addition, the experimental results have also highlighted how the considered test conditions have not significantly affected the general operating of such systems (in other words, a new calibration is not required after the test) and the stresses applied have not damaged the adopted devices.

Future developments will concern with the design of suitable test bed and measurement procedure for a deeper metrological performance analysis of IMUs devices with the aim of providing to final users of IMUs, important additional information about their behaviour under dynamic operating conditions.

REFERENCES

[1] J. Kim, N. D. Thang, and T. Kim, "3-d hand motion tracking and gesture recognition using a data glove," in 2009 IEEE International Symposium on Industrial Electronics, pp. 1013–1018, July 2009.

[2] G. Dissanayake, S. Sukkarieh, E. Nebot, H. Durrant-Whyte, "The aiding of a low-cost strapdown inertial measurement unit using vehicle model constraints for land vehicle applications" *IEEE Transactions on Robotics and Automation* Vol.17 , Issue: 5 , Oct 2001.

[3] K. Keunecke, G. Scholl, "Accurate Indoor Localization by Combining IEEE 802.11 g/n/ac WiFi-Systems with Strapdown Inertial Measurement Units", GeMiC 2014; German Microwave Conference.

[4] Z.Cao, S. Su, H. Chen, H. Tang, Y. Zhou, Z. Wang, "Pose measurement of Anterior Pelvic Plane based on inertial measurement unit in total hip replacement surgeries", 2016 38th Annual International Conference of the IEEE Engineering in Medicine and Biology Society (EMBC).

[5] S. Yosi, N. J. Agung, S. Unang, "Tilt and heading measurement using sensor fusion from inertial measurement unit", 2015 International Conference on Control, Electronics, Renewable Energy and Communications (ICCEREC).

Table 4. Summary of sensors output for Modules A, B and C (the vibration is applied on the x-axis).

		Acc X [g RMS]			Gyro Y [mdps RMS]			Acc Y [g RMS]			Gyro X [mdps RMS]		
		Z_1	Z_2	Z_3	Z_1	Z_2	Z_3	Z_1	Z_2	Z_3	Z_1	Z_2	Z_3
A	**μ**	0.0024	2.2370	0.0022	0.091	8.492	0.095	0.0017	0.2329	0.0017	0.126	0.983	0.124
	σ	0.0002	0.2587	0.0002	0.017	1.025	0.007	0.0002	0.0267	0.0002	0.011	0.120	0.012
B	**μ**	0.0025	2.3456	0.0021	0.096	9.654	0.106	0.0023	0.2592	0.0019	0.106	1.054	0.136
	σ	0.0003	0.3652	0.0004	0.001	1.854	0.010	0.0003	0.0389	0.0003	0.012	0.253	0.014
C	**μ**	0.0031	2.5137	0.0030	0.079	11.179	0.114	0.0009	0.1975	0.0010	0.097	1.211	0.180
	σ	0.0004	0.4804	0.0005	0.007	2.1513	0.016	0.0001	0.0346	0.0001	0.009	0.224	0.016

[6] B. Alandry, L. Latorre, F. Mailly, P. Nouet, "A CMOS-MEMS Inertial Measurement Unit", SENSORS, 2010 IEEE.

[7] D. Capriglione, M. Carratu, P. Sommella, and A. Pietrosanto, "ANN-based IFD in motorcycle rear suspension," in 15th IMEKO TC10 Workshop on Technical Diagnostics 2017 - "Technical Diagnostics in Cyber-Physical Era", pp. 22–27, 2017.

[8] D. Capriglione, M. Carratù, A. Pietrosanto and P. Sommella, "Online Fault Detection of Rear Stroke Suspension Sensor in Motorcycle," in IEEE Transactions on Instrumentation and Measurement, vol. 68, no. 5, pp. 1362-1372, May 2019. doi: 10.1109/TIM.2019.2905945

[9] M. Carratù, A. Pietrosanto, P. Sommella and V. Paciello, "Velocity prediction from acceleration measurements in motorcycle suspensions," 2017 IEEE International Instrumentation and Measurement Technology Conference (I2MTC), Turin, 2017, pp. 1-6. doi: 10.1109/I2MTC.2017.7969943

[10] D. Capriglione, M. Carratù, A. Pietrosanto and P. Sommella, "NARX ANN-Based Instrument Fault Detection in Motorcycle," Measurement Journal, Volume 117, Pages 304-311, March 2018, doi: 10.1016/j.measurement.2017.12.026.

[11] D. Capriglione, M. Carratù, C. Liguori, V. Paciello, and P. Sommella, "A Soft Stroke Sensor for Motorcycle Rear Suspension," Measurement Journal, Vol. 106, pp. 46–52, doi: 10.1016/j.measurement.2017.04.011.

[12] S. Sabatelli, M. Galgani, L. Fanucci, and A. Rocchi, "A double-stage kalman filter for orientation tracking with an integrated processor in 9-d imu," IEEE Transactions on Instrumentation and Measurement, vol. 62, pp. 590–598, March 2013.

[13] D. Bereska, K. Daniec, W. Ilewicz, K. Jędrasiak, R. Koteras, A. Nawrat, M. Pacholczyk, "Influence of temperature on measurements of 3-axial accelerometers and gyroscopes: Embedded into inertial measurement unit", 2016 International Conference on Signals and Electronic Systems (ICSES).

[14] https://www.st.com/en/evaluation-tools/nucleo-f401re.html

[15] https://www.raspberrypi.org/products/raspberry-pi-3-model-b/

[16] Automotive Electronics Council, "Failure Mechanism Based Stress Test Qualification for Integrated Circuit." AEC - Q100 - Rev-H, 2014.

[17] Ahari, A. Viehl, O. Bringmann, and W. Rosenstiel, "Mission profile-based assessment of semiconductor technologies for automotive applications," *Microelectron. Reliab.*, vol. 91, pp. 129–138, Dec. 2018.

[18] K. Choi, D.-Y. Yu, S. Ahn, K.-H. Kim, J.-H. Bang, and Y.-H. Ko, "Joint reliability of various Pb-free solders under harsh vibration conditions for automotive electronics," *Microelectron. Reliab.*, vol. 86, pp. 66–71, Jul. 2018.

[19] W. Merlijn van Spengen, "MEMS reliability from a failure mechanisms perspective," *Microelectron. Reliab.*, vol. 43, no. 7, pp. 1049–1060, Jul. 2003.

[20] D. M. Tanner *et al.*, "MEMS Reliability : Infrastructure, Test structures, Experiments and Failure Modes," *Sandia Report*, no. January. Sandia National Laboratories, 2000.

[21] M. Tilli, T. Motooka, V.-M. Airaksinen, S. Franssila, M. Paulasto-Krockel, and V. Lindroos, *Handbook of Silicon Based MEMS Materials and Technologies*, Second. Elsevier, 2015.

[22] Y. Huang, A. Sai Sarathi Vasan, R. Doraiswami, M. Osterman, and M. Pecht, "MEMS Reliability Review," *IEEE Trans. Device Mater. Reliab.*, vol. 12, no. 2, pp. 482–493, Jun. 2012.

[23] IEC 60068-2-64, "Environmental testing - Part 2: Tests - Test Fh: Vibration, broadband random and guidance." International Electrotechnical Commission, 2012.

[24] ISO 16750-3, "Road vehicles - Environmental conditions and testing for electrical and electronic equipment - Part 3: Mechanical loads." International Organization for Standardization, 2003.

[25] FIAT Group, "Environmental Test Specification - Electronic Components," 2009.

[26] MIL-STD-810G, "Environmental Engineering Considerations and Laboratory Tests," no. October. US Department of Defense, Whasington DC, 2008.

[27] European Telecommunications Standards Institute, "Environmental Engineering (EE); Environmental conditions and environmental tests for telecommunications equipment; Part 2-5: Specification of environmental tests; Ground vehicle installations." ETSI EN 300 019-2-5, 2002.

[28] JEDEC Solid State Technology, "JEDEC STANDARD: Vibration, Variable Frequency." JESD22-B103B.01, 2016.

[29] A. Rossi et al., "A preliminary performance validation of a MEMS accelerometer for blade vibration monitoring," 22nd IMEKO TC4 Int. Symp. 20th Int. Work. ADC Model. Test. 2017 Support. World Dev. Through Electr. Electron. Meas., pp. 180–184, 2017.

[30] M. Catelani, L. Ciani, and A. Reatti, "Critical components test and reliability issues for photovoltaic inverter," in 20th IMEKO TC4 Symposium on Measurements of Electrical Quantities: Research on Electrical and Electronic Measurement for the Economic Upturn, Together with 18th TC4 International Workshop on ADC and DCA Modeling and Testing, IWADC 2014, 2014, pp. 592–596.